# Type VII Collagen in the Human Accommodation System

Wullink, Bart; Pas, Hendri H.; Van der Worp, Roelofje J.; Schol, Martin; Janssen, Sarah F.; Kuijer, Roel; Los, Leonoor I.

*Published in:*
Investigative ophthalmology & visual science

*DOI:*
10.1167/iovs.17-23425



*Publication date:*
2018

# Type VII Collagen in the Human Accommodation System: Expression in Ciliary Body, Zonules, and Lens Capsule

Bart Wullink,[1,2] Hendri H. Pas,[3] Roelofje J. Van der Worp,[1,2] Martin Schol,[1] Sarah F. Janssen,[4,5] Roel Kuijer,[2,6] and Leonoor I. Los[1,2]

[1]Department of Ophthalmology, University Medical Center Groningen, University of Groningen, Groningen, The Netherlands
[2]W.J. Kolff Institute, Graduate School of Medical Sciences, University of Groningen, Groningen, The Netherlands
[3]Department of Dermatology, University Medical Center Groningen, University of Groningen, Groningen, The Netherlands
[4]Department of Ophthalmology, VU Medical Center, Amsterdam, The Netherlands
[5]Department of Clinical Genetics, Academic Medical Center, Amsterdam, The Netherlands
[6]Department of Biomedical Engineering, University Medical Center Groningen, University of Groningen, Groningen, The Netherlands

Correspondence: Bart Wullink, Department of Ophthalmology, University Medical Center Groningen, University of Groningen, Hanzeplein 1, P.O. Box 30001, Groningen 9700RB, The Netherlands; b.wullink@umcg.nl.

Submitted: November 17, 2017
Accepted: January 16, 2018

Citation: Wullink B, Pas HH, Van der Worp RJ, et al. Type VII collagen in the human accommodation system: expression in ciliary body, zonules, and lens capsule. *Invest Ophthalmol Vis Sci*. 2018;59:1075–1083. https://doi.org/10.1167/iovs.17-23425

**Purpose.** To investigate intraocular expression of COL7A1 and its protein product type VII collagen, particularly at the accommodation system.

**Methods.** Eyes from 26 human adult donors were used. COL7A1 expression was analyzed in ex vivo ciliary epithelium by microarray. Type VII collagen distribution was examined by Western blot analysis, immunohistochemistry. and immuno-electron microscopy.

**Results.** COL7A1 is expressed by pigmented and nonpigmented ciliary epithelia. Type VII collagen is distributed particularly at the strained parts of the accommodation system. Type VII collagen was associated with various basement membranes and with ciliary zonules. Anchoring fibrils were not visualized.

**Conclusions.** Type VII collagen distribution at strained areas suggests a supporting role in tissue integrity.

Keywords: collagen type VII, inner limiting membrane, basement membrane, accommodation, lens capsule

Type VII collagen (Col VII) is renowned as the major component of anchoring fibrils.[1] It is essential for epithelium-to-stroma anchorage in skin, mucosa, and cornea.[2,3] Although predominantly expressed in skin, Col VII is estimated to comprise a mere 0.001% of the total skin collagen content.[4] Yet, the relevance of such levels of Col VII expression is clinically evidenced in severe dystrophic epidermolysis bullosa, in which patients lack functional Col VII (i.e., anchoring fibrils). Their skin blisters readily at small amounts of friction, damaging their epithelial basement membranes at each event. Such repetitive wounding is accompanied by severe and extensive scar formation, mutilating deformations, and recurrent infections. Patients succumb to skin cancer or sepsis often before age 35.[5,6] Extraocular manifestations are well documented, and encompass mainly corneal and conjunctival (both surface ectoderm) erosions accompanied by scar formation, symblepharon, pannus, and so forth.[6] Intraocular manifestations are mentioned only in rare case reports, where no clinical or histological abnormalities are found,[7] or are limited to lens (also surface ectoderm) sclerosis.[7–9] Interestingly, however, retinal COL7A1 gene expression was recently established (FANTOM5 consortium[10]). Moreover, its protein product was demonstrated at the vitreoretinal junction[11,12] and inner layers of the normal retina,[12,13] although no anchoring fibrils were visualized. Anchoring fibrils, however, are reported to be far more numerous at basement membrane zones of mechanically strained tissues.[2,14,15] To investigate the characteristics of intraocular Col VII further, we explored the accommodation system. We observed COL7A1 expression at the pigmented and nonpigmented ciliary epithelia, and Col VII protein at the ciliary body and zonules.

## Materials and Methods

### Samples

Eyes were provided by the Euro Cornea Bank, Beverwijk (http://www.eurotissuebank.nl/corneabank/, in the public domain), The Netherlands. In The Netherlands, the usage of donor material is provided for by the Organ Donation Act (Wet op de orgaandonatie [WOD]). In accordance with this law, donors provide written informed consent for donation, with an opt-out for the usage of leftover material for related scientific research. Specific requirements for the use in scientific research of leftover material originating from corneal grafting have been described in an additional document formulated by the Ministry of Health, Welfare, and Sport, and the BIS Foundation (Eurotransplant; Leiden, July 21, 1995; 6714.ht). The current research was carried out in accordance with all requirements stated in the WOD and the relevant documents. Approval of the local medical ethics committee was not required, because the data were analyzed anonymously. Skin tissue was obtained from a cosmetic surgery procedure, after written informed consent of the patient and approval by the institutional review board.

**Table 1.** Donor Characteristics

| Assay | Embedding | Age | Sex | Cause of Death | Comorbidity | Fixative |
|---|---|---|---|---|---|---|
| IHC | Paraffin | 83 | Female | Cerebrovascular accident | Polymyalgia rheumatica | 2% PF |
| | | 65 | Male | Cardial | Bladder cancer | 2% PF |
| | | 64 | Male | Cardial | | 2% PF |
| | | 78 | Female | Cerebrovascular accident | | 2% PF |
| | Cryo | 67 | Female | Malignancy | | None |
| | | 68 | Male | Malignancy | | None |
| | | 83 | Male | Cardial | | None |
| | | 35* | Female | N/A (control, abdominal skin) | Obesity | None |
| | T8100 | 78 | Male | Lung cancer | | 2% PF |
| | | 69 | Female | Cerebrovascular accident | | 2% PF |
| | | 66 | Male | Cardial | | 2% PF |
| | | 35 | Male | Cardial | | 2% PF |
| iTEM | T8100 | 56 | Male | Cardial (suicide) | | 2% PF |
| | | 77 | Male | Cardial | Atrial fibrillation | 2% PF |
| | | 78 | Female | Cardial (asystole) | Vascular disease | 2% PF |
| Western blot | | 63 | Male | Trauma | | None |
| | | 78 | Female | Cerebrovascular accident | | None |
| | | 44 | Female | Suicide | Intoxication | None |
| | | 56 | Female | Malignancy | | None |
| Gene expression | Cryo | 39 | Male | Cardial | | None |
| | | 48 | Female | Cardial | | None |
| | | 56 | Male | Aortic dissection | | None |
| | | 58 | Male | Cardial | | None |
| | | 68 | Male | Cerebrovascular accident | Hypertension | None |
| | | 70 | Female | Cardial | | None |
| | | 73 | Male | Cardial | | None |

PF, paraformaldehyde.
* Skin sample only.

We analyzed eyes from a total of 26 human donors (age 35–83 years, mean age 63.7 years), which were without known ophthalmic pathology (Table 1). In general, corneas had been removed for transplantation purposes. All eyes were fixed, frozen, or processed within 48 hours postmortem.

## Embedding

Eleven eyes were embedded in paraffin or resin as described previously.[12] For light microscopy, the anterior parts of four eyes were positioned in 2% agarose before paraffin embedding, and sectioned at 3 to 4 μm (Leica RM2265; Microtome, Heidelberg, Germany). For electron microscopy, the anterior parts of three eyes were washed, dehydrated, pre-infiltrated, and embedded in T8100 resin (Technovit 8100; Heraeus Kulzer, Wehrheim, Germany). Areas of interest were sawn out, trimmed and sectioned at 100-nm thickness (Ultracut type 701; Reichert-Jung, Vienna, Austria). Three eyes and a skin sample were not fixed, but mounted in optimal cutting temperature compound (Tissue-Tek; Sakura Finetek Europe, Alphen aan den Rijn, The Netherlands), snap-frozen in isopentane propane in liquid nitrogen, and cut in 7- to 10-μm thick sections (CM3050 S Cryostat; Leica Microsystems, Wetzlar, Germany).

## Immunohistochemistry

Paraffin, T8100, and cryosamples were processed as described previously.[12] In short, sections from four paraffin-embedded eyes were deparaffinized with xylene followed by ethanol rehydration steps. After washing, a protease K (IHC Select kit; Chemicon/Millipore, Billerica, MA, USA) dilution of 1:5 in PBS was added for 15 minutes to unmask epitopes. After washing, endogenous peroxidases were blocked (0.3% $H_2O_2$/PBS for 30 minutes). Nonspecific binding of antigens was prevented (3% BSA/PBS for 30 minutes). Primary anti-Col VII antibodies (Supplementary Table S1) were allowed to incubate (1:100 in PBS for 1 hour). These comprised two monoclonal antibodies, designated mAb(12) (LH7.2; Abcam, Cambridge, UK) and mAb(14) (clone 32; EMD Millipore, Billerica, MA, USA) and two polyclonal antibodies, designated pAb(16) (anti-tissue type Col VII; Calbiochem, San Diego, CA, USA) and pAb(72) (recombinant LH7.2, a kind gift from Alex Nyström, PhD, University of Freiburg, Freiburg im Breisgau, Germany). After thorough washing in PBS, sections were incubated in corresponding horseradish conjugated secondary antibodies (rabbit-anti-mouse and goat-anti-rabbit; DAKO, Glostrup, Denmark) (1:500 in PBS for 1 hour). Sections were washed, then stained using 3-amino-9-ethylcarbazole (AEC Staining Kit; Sigma-Aldrich, St. Louis, MO, USA) and counterstained with hematoxylin. For signal enhancement, an avidin/biotin labeling kit was used (Vectastain Elite ABC kit; Vector Labs, Burlingame, CA, USA), according to the manufacturer's instructions. An HC DMR microscope (Leica) was used to analyze the samples. All proceedings were performed at room temperature. In negative control sections, incubation with primary antibodies was omitted.

## Immuno-Electron Microscopy

Sections from T8100 embedded eyes were mounted on 150-mesh, 0.6% formvar-coated nickel grids. For antigen retrieval, samples were incubated in 0.05% trypsin (Gibco, Paisley, Scotland) in 0.1 M Tris-buffer (pH 7.8) containing 0.1% $CaCl_2$, for 15 minutes at 37°C. The sections were washed in 0.2 M phosphate buffer, incubated in 0.1 M citric acid (pH 3.0) for 30 minutes at 37°C, and washed again. To block nonspecific binding of the primary antibody, sections were incubated in PBS containing 2% BSA-c (Aurion, Wageningen, The Netherlands) and 2% goat serum, for 30 minutes at room temperature.

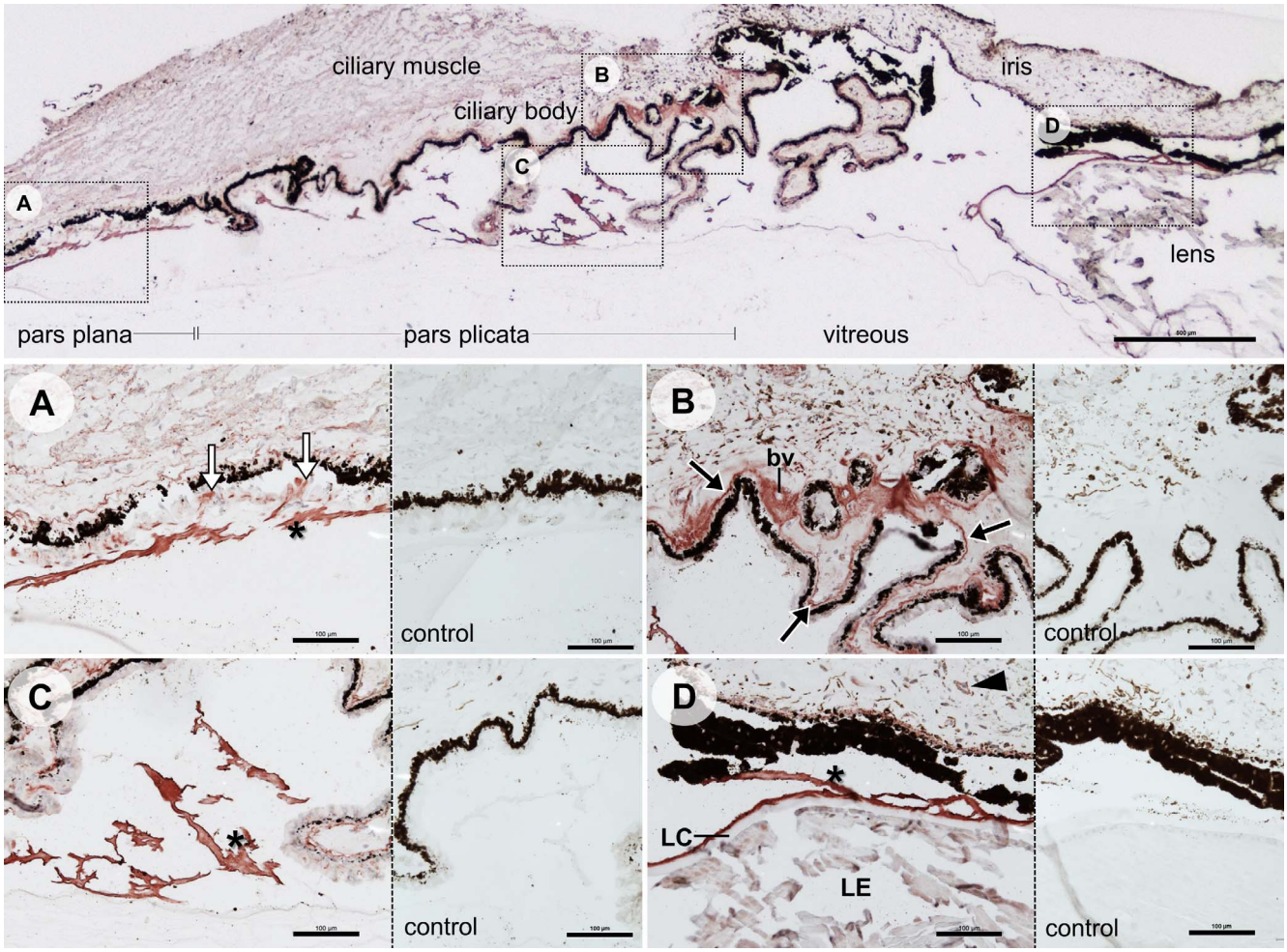


**Figure 1.** Col VII labeling of the accommodation system; pAb(16). Overview. *Scale bar*: 500 μm. (**A**, **C**, **D**) Zonules (*) label intensely, as do their probable sites of origin at the nonpigmented epithelium layer (*white arrows*). (**B**) Linear labeling is observed at the basement membrane of the ciliary pigmented epithelium. At the bases of the ciliary processes, extensive labeling is observed around blood vessels (*black arrows*). (**D**) The lens (LE) and its capsule (LC) appear unlabeled, in contrast to zonules (*), iris blood vessels (*arrowhead*) and the basement membrane of iris pigmented epithelium. Controls did not label. *Scale bars*: 100 μm.

Sections were then incubated in primary antibody pAb(16) (1:100) in a 1% BSA-c/PBS buffer, initially for 2 hours at 37°C, then at room temperature overnight. Afterward, the sections were washed, and incubated with gold-labeled anti-rabbit IgG (goat-anti-rabbit, Gold Colloid 6 nm, 1:200; Aurion) for 1 hour. The samples were washed in ultrapure water, fixed in 2% glutaraldehyde for 2 minutes, silver-enhanced according to kit protocol (R-Gent SE-LM Silver enhancement kit; Aurion) for 10 minutes at room temperature, and washed again with ultrapure water. Then, they were contrasted by applying methylcellulose-uranyl acetate (9:1) at 4°C for 15 minutes, after which the solution was removed. The samples were allowed to dry for at least 15 minutes, and were analyzed in a CM100 BioTwin transmission electron microscope (TEM) (Philips, Eindhoven, The Netherlands) using immuno-electron microscopy (iTEM) software (ResAlta Research Technologies, Golden, CA, USA) and a Morada 11-MP TEM camera (Olympus Soft Imaging Solutions GmbH, Münster, Germany).

## Antibody Epitope Mapping

The antibodies mAb(12), mAb(70) (US Biological, Swampscott, MA, USA), and pAb(72) target Col VII at its amino terminus (NC-1), whereas mAb(14) targets the collagenous domain toward the amino-terminal end. To assess the target epitopes of pAb(16), this antibody was mapped by a third party commercial laboratory (PEPperPRINT, Heidelberg, Germany) (Supplementary Fig. S1).

## Western Blotting

Seven bulbi (three pairs pooled for pAb[16], one bulbus for mAb[14]) were microscopically dissected in cooled 90% glycerol (diluted in 1% EDTA/PBS). Their anterior segment was isolated by cutting through the pars plana of the ciliary body circumferentially. The vitreous was dissected close to the anterior hyaloid, the iris was bluntly removed by forceps. The anterior segment was stretched and fixed on a clear silicone layer by insect pins. The zonules and lens capsule were contrasted with MembraneBlue-Dual dye (DORC, Zuidland, The Netherlands). The zonules were cut closely to the inner limiting membrane (ILM), minimizing contamination by ILM and ciliary epithelium. After opening of the capsular bag and removing the lens, visible lens fibers were flushed out. Traces of iris pigment that stuck to the anterior lens capsule were removed with Q-tips. Then, the pars plicata of the ciliary body was isolated from remaining retinal and choroidal fragments. Excess fluids were removed by centrifugation (85 *g* for 2 minutes). Tissues were homogenated by turraxing them in 0.5% Triton X-100 in Tris-buffered saline. Some samples were

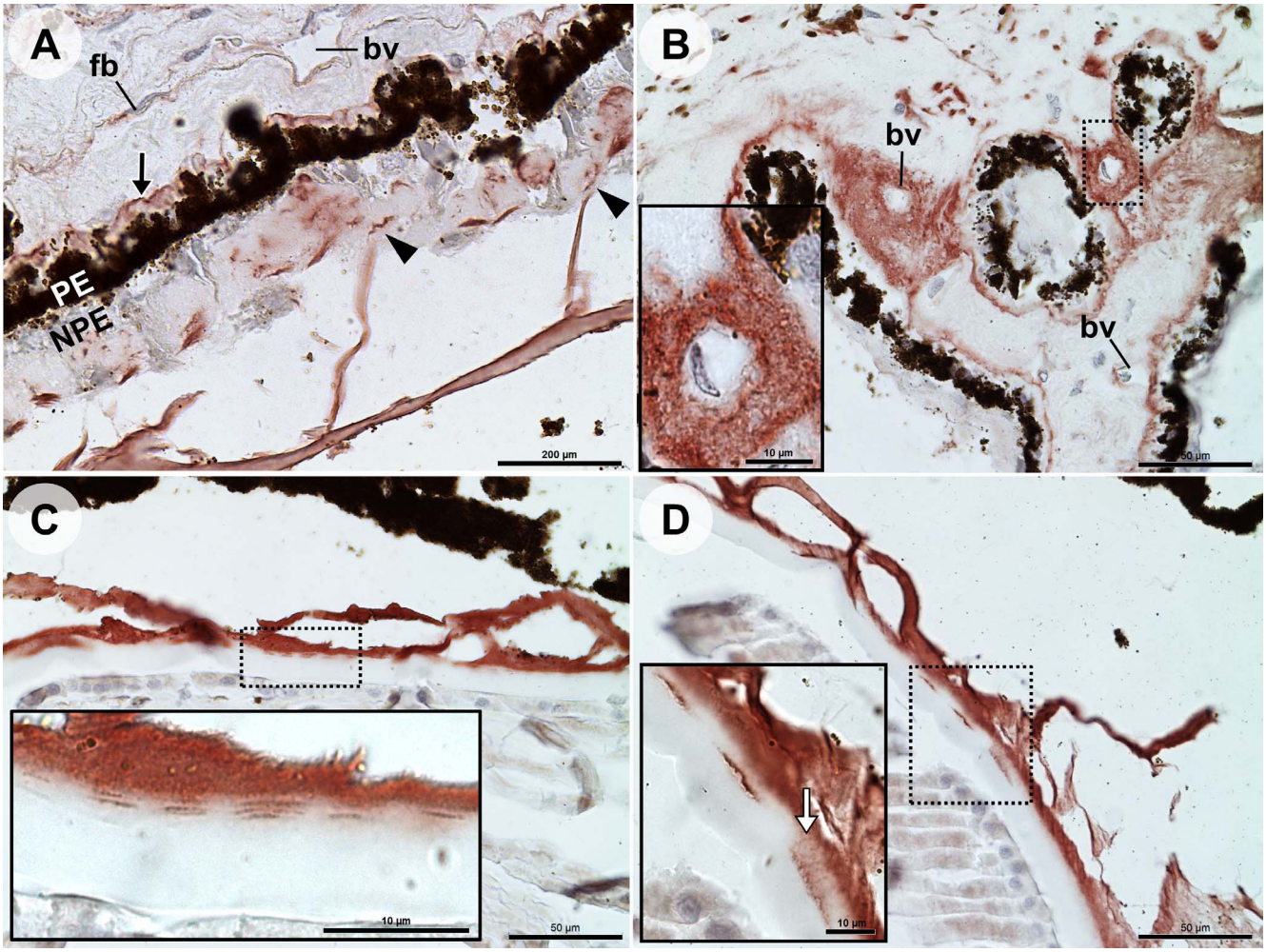


FIGURE 2. Col VII labeling of the ciliary body and zonules; pAb(16). Higher magnification of Figure 1. (**A**) Pars plana. The zonules connect to fibrillar structures (*arrowheads*) in the ILM, which locally invaginates the NPE. Apart from the fibrillar structures, the ILM does not label. Linear labeling is observed at the basement membrane (*black arrow*) of the PE. Mostly, stromal fibroblasts (fb) display labeling, whereas small blood vessels (bv) do not. *Scale bar*: 200 µm. (**B**) Pars plicata. The larger blood vessels, at the bases of the ciliary processes, label broadly in contrast to other blood vessels (bv). *Scale bar*: 50 µm (*inset bar*: 10 µm). (**C**, **D**) Antero-equatorial lens capsule. Superficial intracapsular structures are labeled, at sites of zonular contact. Some fibrillar labeling is seen between a zonule contact point and an underlying intracapsular structure (*white arrow*). *Scale bars*: 50 µm (*inset bar*: 10 µm).

subjected to bacterial type VII collagenase (high purity grade, 30 units for 1 hour at 37°C; Sigma, City, State, Country) or pepsin (vortexing 5 minutes at room temperature, 4 mg/mL pepsin in 0.5 M acetic acid at one-fourth sample volume; Sigma) digestion before sample buffer incubation. Sample buffer, SDS-PAGE, and Western blotting were performed as described earlier.[12] Briefly, nitrocellulose membranes were blocked with 2% fat-free milk and incubated overnight in mAb(14) or pAb(16) (Supplementary Table S1). The membranes were incubated in corresponding secondary antibodies (goat-anti-mouse or goat-anti-rabbit; Jackson ImmunoResearch, West Grove, PA, USA), washed, incubated in tertiary alkaline phosphatase-conjugated antibodies (rabbit-anti-goat-AP; Jackson ImmunoResearch) for 1 hour each, and developed with NBT/BCIP (BioRad, Hercules, CA, USA). All steps were performed at RT. In controls, the primary antibody was omitted.

### Gene Expression

To assess COL7A1 expression in pigmented epithelium (PE) and nonpigmented epithelium (NPE), gene expression level data were provided by Janssen et al.[16] Data were derived from their total dataset, including the unpublished remainder of their selection of top 10% relevant PE and NPE genes. In short, PE and NPE cells from seven snap-frozen donor samples were separately collected through laser dissection microscopy. Then, RNA isolation, amplification, labeling, and hybridization against 44×k Agilent microarrays was performed. Gene expression data were analyzed with R and the knowledge database Ingenuity.[16]

## RESULTS

### Immunohistochemistry (IHC) and iTEM: Polyclonal Antibody

By light microscopy, pAb(16) labeling was observed at the ciliary zonules, stromal fibroblasts, and the basement membranes of PE and blood vessels. The zonules showed anti-Col VII labeling along their entire span (Figs. 1, 2). Through that labeling, zonules could be traced to fibrillar structures at the NPE layer (Figs. 1A, 2A). Labeling of the PE basement membrane was sharply delineated from pars plana (Fig. 1A)

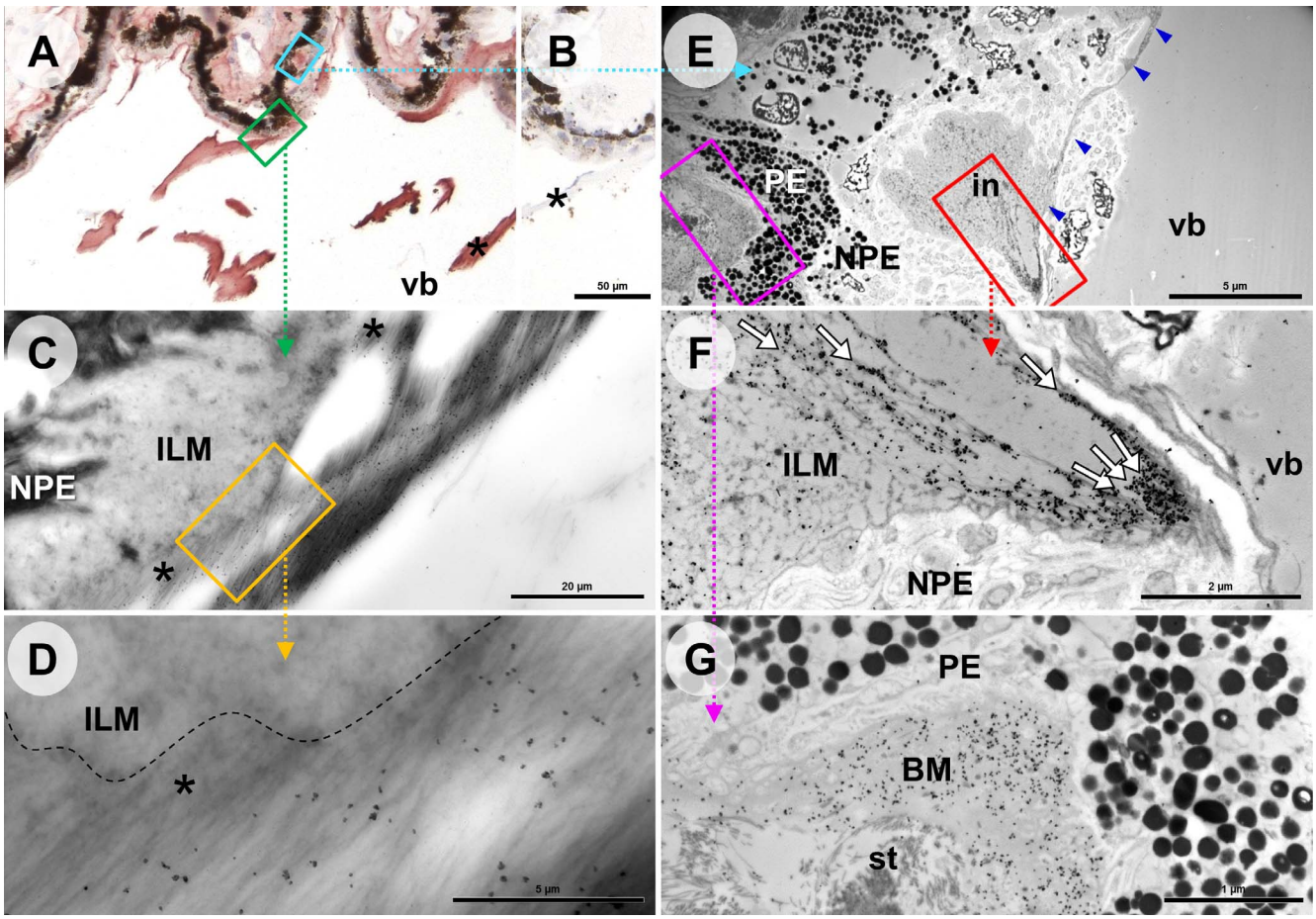


FIGURE 3. Col VII gold labeling of the zonules and basement membranes of PE and NPE; pAb(16). (**A**) Light microscopic overview. (**B**) Negative control. *Scale bar*: 50 µm. (**C**) iTEM: Zonular fibers (*) are homogeneously labeled (*black dots*). The ILM is not labeled. *Scale bar*: 20 µm. (**D**) A zonule adjacent to the ILM; no (fibrillar) zonule-ILM interactions are apparent. *Scale bar*: 5 µm. (**E**) Labeling at the basement membrane zone of the PE and at sites of zonular insertion (*in*) (or ILM invagination) into the NPE. Outside the invaginations, the ILM is a thin, practically unlabeled sheet (*arrowheads*). *Scale bar*: 5 µm. (**F**) Individual fibrils derive from the peripheral areas of the invaginated ILM and aggregate into a fiber (*white arrows*). *Scale bar*: 2 µm. (**G**) At this cutting angle, the gold-labeled basement membrane (BM) of the PE appears broad. No anchoring fibrils are visualized between the BM and the subjacent unlabeled stroma (st). *Scale bar*: 1 µm.

to pars plicata. However, at the bases of the ciliary processes (Fig. 1B), the area in-between the PE basement membrane and that of nearby blood vessels labeled broadly (i.e., Figs. 1B, 2B). Such labeling around blood vessels diminished rapidly toward the tips of the ciliary processes, where the sharp delineation returned (Fig. 1C). The lens and lens capsule remained unlabeled (Fig. 1D). At higher magnification, however, small intracapsular structures were seen at the antero- and post-equatorial capsule, where they corresponded to zonules (Figs. 2C, 2D). They disappeared toward the anterior and posterior poles. The basal lamina of the posterior iris PE was slightly labeled, posteriorly more so than anteriorly. The iris stroma showed almost no labeling. Lens fibers showed some faint background labeling (on rare occasion), and were considered "unlabeled" (Fig. 1D).

By iTEM, such IHC labeling was confirmed. The zonules, including their NPE origin and capsular insertions, were labeled, as was the basement membrane of PE. No anchoring fibrils could be distinguished (Figs. 3, 4). The basement membrane of the PE labeled moderately throughout its entire thickness (Figs. 3E, 3G).

At the capsular surface, some approximating zonules extended protruding fibrils, perpendicular to the zonular course and lens capsule surface (Fig. 4E). Here, the assembled zonules ran parallel to the capsular surface, thus forming the zonular lamella. At areas without such perpendicular fibrils, a lucid unlabeled plane was seen between the zonules and lens capsule (Fig. 4D; Supplementary Fig. S2). Intracapsular densities (or linear densities)[17] were readily distinguishable from the lens capsular bulk by contrast density, but moreover, because they were the only capsular structures that were labeled (Fig. 4D). Although the labeled densities could indent the lens epithelial surface (Supplementary Fig. S2B), no actual intracellular labeling was seen. The intracapsular densities had round or elongated (linear) shapes. Their fibrillar aspect and labeling were less outspoken than that of zonules (Figs. 4C, 4D). The round densities had lucent envelopes, which were less distinct in the elongated variant (Figs. 4C, 4D; Supplementary Fig. S2B). At the (antero-) equatorial lens capsule zonular fibrils mingled with the capsule at certain points (Fig. 4E), but otherwise paralleled a lucent superficial capsular plane (Supplementary Figs. S2A, S2B). No connections between zonules and intracapsular densities could be visualized convincingly, although on occasion faint intermediary fibrillar shapes could be discerned (Supplementary Fig. S2C). The NPE and PE cells labeled negligibly, as did the collagenous stroma underneath the PE. In both IHC and iTEM, the vitreous cortex, the lens fibers, and the lens epithelium

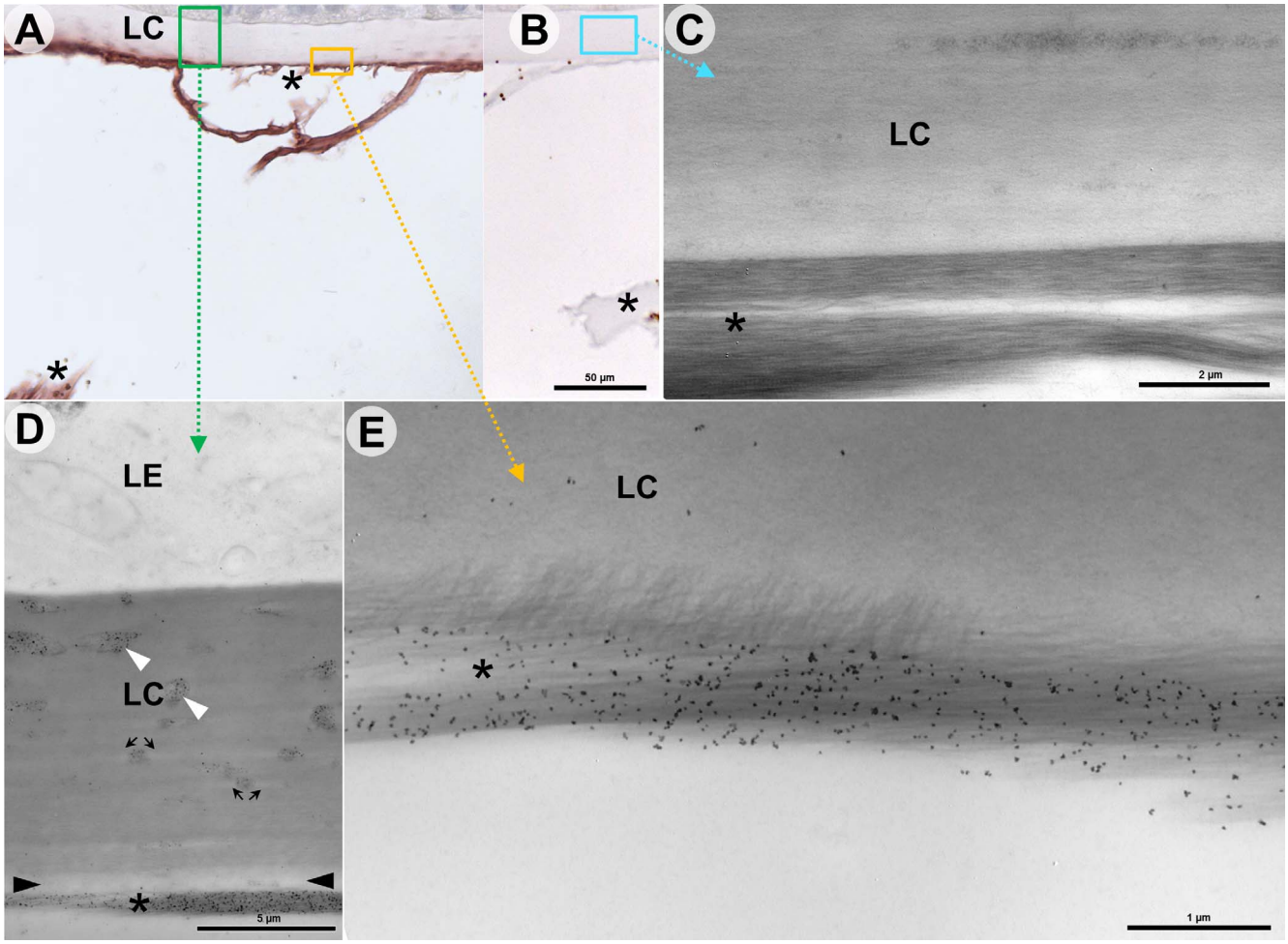


FIGURE 4. Col VII labeling of the zonules and their capsular insertions; pAb(16). (**A**) Light microscopic overview. The labeled intracapsular densities are most prominent underneath zonular attachments (*). (**B**) Negative control. *Scale bar*: 50 µm. (**C**) Negative control iTEM. *Scale bar*: 2 µm. (**D**) iTEM: Intracapsular densities also reside deep in the lens capsule (*white arrowheads*), but the lens epithelium (LE) is unlabeled. A lucid layer is seen between zonules and lens capsule, at the antero-equatorial region (*black arrowheads*). The lens capsule has a striated aspect. Round linear densities are often flanked by an elongated area of lesser contrast (*small black arrows*). *Scale bar*: 5 µm. (**E**) iTEM: Perpendicular zonular fibers intermingle with the antero-equatorial lens surface, which is more lucent than its deeper parts. *Scale bar*: 1 µm.

TABLE 2. Summary of pAb(16) Labeling Intensities, Semi-Quantitative Col VII Determination

| | Wb | IHC | iTEM |
|---|---|---|---|
| Ciliary body | + | | |
| Stroma (fibroblasts) | | + | + |
| Vascular BM | | ++ | + |
| PE BM | | +++ | ++ |
| NPE BM (ILM) | | - | - |
| Intercellular zonular origins | | ++ | ++ |
| Zonules/lens capsule complex | + | | |
| Zonules | | +++ | +++ |
| Lens capsule | | | |
| Zonular membrane | | - | - |
| Linear densities | | ++ | ++ |
| Lens | - | - | - |

BM, basement membrane; -, no signals; +, weak; ++, moderate; +++, intense.

remained unlabeled. Negative controls (IHC/iTEM) had no significant labeling or background. Results are summarized in Table 2.

## Antibody Epitope Mapping

Seven epitopes could be identified on the pAb(16) antibody with specific binding affinity for Col VII. The three epitopes with the best signal-to-noise ratio (E-value), had affinity for the collagenous triple helical domain of Col VII. Of the four remaining epitopes, two epitopes would target NC-1 peptide sequences in the fibronectin (FN3) domain and two in the von Willebrand factor (vWFA) domain (Supplementary Fig. S1).

## IHC and iTEM: Confirmation Antibodies

To confirm our immunohistochemical results obtained by pAb(16) in ocular tissues, a comparison with other validated antibodies was made in cryosections of skin (Supplementary Fig. S3) and ciliary body (Fig. 5). All antibodies labeled the dermal-epidermal basement membrane zone specifically. In cryosections of ocular tissue, the labeling of the pAb(16) antibody was partially reproduced by the other antibodies. The zonular fragments that survived cryosectioning were stained

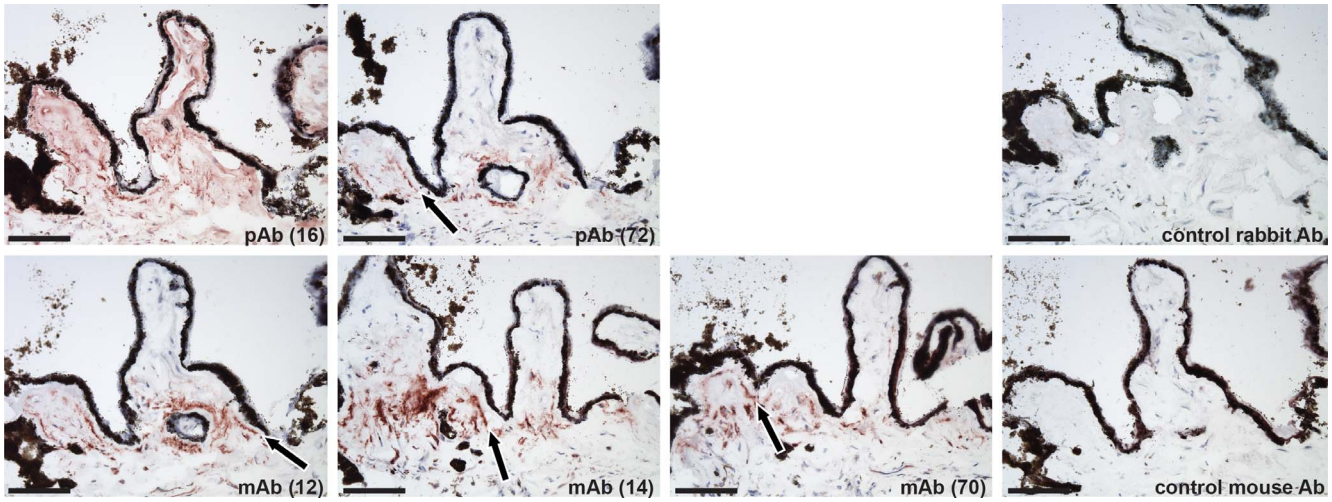


FIGURE 5. Anti-Col VII antibody comparison on unfixed ciliary body cryosections. The five antibodies label at the bases of the anterior ciliary processes, whereas the signal is more reduced at the posterior processes. The extensive labeling by the pAb(16) antibody is partially reproduced by the other antibodies. Here, pAb(16) gives more background labeling than in the paraffin sections (see Figs. 1, 2). There is some longitudinal staining, which indicates basement membrane associated staining (*arrows*). The few zonular fragments that remained after sectioning were stained faintly by the pAb(16) antibody, but not by the other antibodies. The linear densities in the lens capsule were not stained. Negative controls showed no signals. *Scale bars*: 100 μm.

faintly, and only by the pAb(16) antibody. Intracapsular densities were not discernible. Avidin-biotin signal enhancement often resulted in basement membrane labeling. Evaluation by iTEM could not be performed, because none of the comparison antibodies proved able to label positive control sections of skin in T8100 adequately.

### Western Blotting

Col VII could be demonstrated in accommodation system lysates by mono- and polyclonal antibodies (Fig. 6). Although Col VII was not easily extracted from cornea control tissue, a limited collagenase digestion of the crude lysate showed a 290-kDa signal. Tissue type Col VII could be detected in zonules/lens capsule and ciliary body lysates, although a brief pepsin treatment of the crude lysate was needed for mAb(14) detection.

### Gene Expression

COL7A1 is equally expressed in PE and NPE at "low" levels (compared with the total dataset), as indicated by a "$\log_2$-

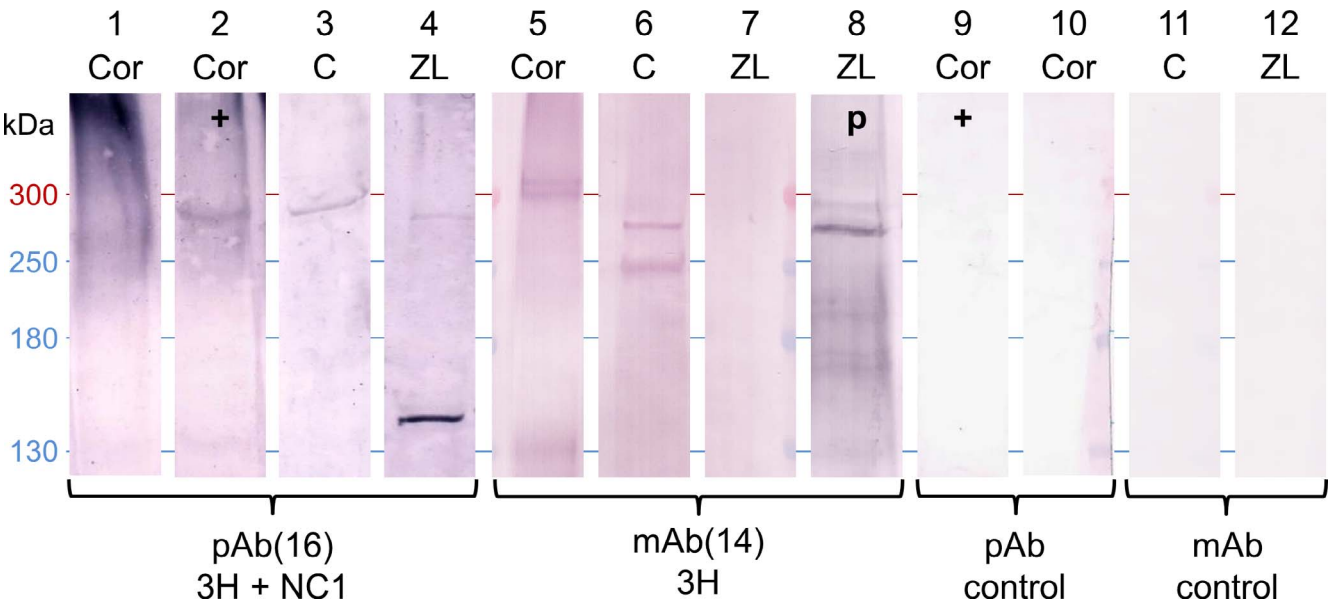


FIGURE 6. Western blots of accommodation system tissue lysates, with several antibodies against type VII collagen. Lanes 1–4. pAb(16): No clear bands are seen in cornea lysates (Cor), which served as a positive control, but high molecular weight aggregates (i.e., anchoring fibrils) are suspected given the dark smear at the top. Limited collagenase digestion (+) of cornea lysates clears the dark smear and results in a band of approximately 290 kDa. This band is also detected in ciliary body (C) and zonule/lens capsule (ZL). Zonule/lens capsule lysates also show a strong band approximately 145 kDa. Lanes 5–8. mAb(14): In another lysate batch, cornea lysates show a signal approximately 320 kDa, the ciliary body lysate approximately 290 and 250 kDa, whereas the zonula/lens capsule lysate only shows bands at 290 and 170 kDa after limited pepsin digestion (p) (compare lane 7 with lane 8). 3H, triple helix; NC1, noncollagenous amino terminal domain, + collagenase; p, pepsin. Lanes 9–12. Negative control samples show no bands.

Investigative Ophthalmology & Visual Science

**Table 3.** Gene Expression Levels of COL7A1 in Microdissected PE and NPE

| Expression Level* | Expression Value |
|---|---|
| Very low/absent | <5.2955 |
| Low | 5.2955–9.0730 |
| Moderate | 9.0730–13.5714 |
| High | >13.5714 |

| Sex | Age | PE | NPE |
|---|---|---|---|
| Male | 39 | 7.40866 | 7.27961 |
| Female | 48 | 8.00464 | 7.52513 |
| Male | 56 | 7.21992 | 7.16688 |
| Male | 58 | 7.76748 | 8.09621 |
| Male | 68 | 7.68512 | 7.91423 |
| Female | 70 | 7.21064 | NA |
| Male | 73 | 7.59679 | 7.84793 |

* The mean gene expression values of the epithelia after normalization range from 2.09 to 18.88 ($log_2$ transformed absolute expression levels). Janssen et al.[16] published the selected "highly expressed genes" group, which mean expression levels ranged from 13.70 to 18.88. COL7A1 expression in ciliary epithelia is approximately 7 to 8, which corresponds to a "low" expression level (compared with the total dataset). Description: mRNA, *Homo sapiens* collagen, type VII, alpha 1 (COL7A1) (epidermolysis bullosa, dystrophic, dominant and recessive). Systematic Name: NM_000094. Age at enucleation.

transformed absolute expression level"[16] (Table 3). These data can be found in the Gene Expression Omnibus database (GSE37957).

## Discussion

This study establishes Col VII expression in accommodation system tissues. Col VII is mainly immunolocated at the zonules, and around the blood vessels at the bases of ciliary processes. COL7A1 mRNA is expressed in human PE and NPE cells, at low levels.

The zonules are "woven" by the NPE during organogenesis,[18] when fine zonular fibers originate at the intercellular spaces of the NPE,[19] aggregate into zonules, and then transverse the ILM. With aging, the ILM is infolded into those intercellular spaces,[19] which corresponds to the "invaginations" we currently describe. Upon their lens capsule penetration, the zonules resolve into broadly fanning microfibrils,[20] which anchor to "poorly defined structures" near the epithelial cells.[21,22] This anchoring fashion withstands the repetitive mechanical strain of accommodation.[21] By Col VII labeling, we underline that the zonules penetrate the lens capsule, transverse intracapsularly, and represent the "linear densities" (Supplementary Fig. S2A) of the anterior and equatorial lens capsule.[17] Col VII might support the microfibrillar interaction at either zonular terminus.

Zonules were labeled by pAb(16) in cryo and paraffin slides, but not by the other antibodies. Because monoclonal antibodies were able to detect Col VII by Western blot, Col VII epitopes might be unavailable when embedded within the zonular matrix, or due to steric hindrance of the antibodies. Because pAb(16) has several binding sites for Col VII, such restrictions may apply to a lesser extent, thus possibly explaining different staining patterns. To assess the origin of zonular Col VII, we obtained microarray data from ex vivo NPE and PE cells. Their COL7A1 mRNA expression profiles, combined with the data from Western blots, add to our IHC results. Our hypothesis of a possible role of Col VII in the accommodation system is therefore supported. The low levels of COL7A1 expression at detectable Col VII protein amounts suggest a low turnover (e.g., in comparison with skin[23]).

The demonstration of Col VII at ciliary stromal cells, PE, and blood vessels might relate to the repetitive mechanical strain these tissues are subjected to. The contact points between PE and the blood vessels at the ciliary base, for example, are intensely labeled. The ciliary epithelia need a rich vasculature for their active secretory functions. Unaided, such vascular accommodation might diminish the structural tenacity of the processes. Interestingly, accommodation system histopathology has not been reported in Col VII–deficient patients.[7,8]

By Western blot, the intense zonular IHC labeling appears to be due to the presence of NC-1 globuli. Although isolation of the relative minute quantities of Col VII from any extracellular matrix can be complicated due to its firm embedding therein, mAb(14) was able to detect a full-length Col VII (290-kDa) signal in zonular/lens capsule lysates. However, none of the mAbs was able to target zonules in sections successfully, in contrast to ciliary body and cornea. Thus, the IHC/iTEM results obtained with pAb(16) could not be completely reproduced with other antibodies. We have tried to validate pAb(16) in various ways. The pAb(16) is frequently used in Col VII investigations, and does not show significant cross-reactivity to Col VII–deficient human[12] or mouse tissues[24] or keratocytes.[25]

Interestingly, convincing anchoring fibrils were not visualized, although some looped shapes of thin fibrils were situated in-between anti–Col VII–labeled structures (Supplementary Fig. S2C). Still, the function of Col VII might be established indirectly, through determination of interacting proteins. Proteomic studies have detected Col VII in human ciliary body,[11] ILM,[11,26] retinal blood vessel,[11] and bovine zonule (Col VII fragment C9JBL3_HUMAN[27]) samples, but the established dermal Col VII interactors (i.e., type I and IV collagen, laminin 332) were detected incompletely (ciliary body,[28,29] zonule,[27] lens capsule[11]). Interactions of Col VII and fibrillin, the main component of zonules and part of a tissue mechanosensing complex,[30] have not been documented.

To address the potential functions of intraocular Col VII further, the discrepancy between Col VII labeling in the absence of anchoring fibrils would be supported by identifying the functional ocular Col VII interactor isotypes and possibly by thorough ophthalmological examination of patients with recessive dystrophic epidermolysis bullosa.

### *Acknowledgments*

The authors thank the Euro Cornea Bank for supplying donor eyes, Behrouz Zandieh-Doulabi from VU University Amsterdam for his scientific assistance, the University Medical Center Groningen (UMCG) Microscopy and Imaging Centre for their equipment, and the UMCG Department of Plastic Surgery for supplying control tissue.

Disclosure: **B. Wullink**, None; **H.H. Pas**, None; **R.J. Van der Worp**, None; **M. Schol**, None; **S.F. Janssen**, None; **R. Kuijer**, None; **L.I. Los**, None

### *References*

1. Sakai LY, Keene DR, Morris NP, Burgeson RE. Type VII collagen is a major structural component of anchoring fibrils. *J Cell Biol*. 1986;103:1577–1586.
2. Keene DR, Sakai LY, Lunstrum GP, Morris NP, Burgeson RE. Type VII collagen forms an extended network of anchoring fibrils. *J Cell Biol*. 1987;104:611–621.
3. Gipson IK, Spurr-Michaud SJ, Tisdale AS. Anchoring fibrils form a complex network in human and rabbit cornea. *Invest Ophthalmol Vis Sci*. 1987;28:212–220.

4. Bruckner-Tuderman L, Schnyder UW, Winterhalter KH, Bruckner P. Tissue form of type VII collagen from human skin and dermal fibroblasts in culture. *Eur J Biochem*. 1987; 165:607–611.
5. Mittapalli VR, Madl J, Löffek S, et al. Injury-driven stiffening of the dermis expedites skin carcinoma progression. *Cancer Res*. 2016;76:940–951.
6. Fine JD, Mellerio JE. Extracutaneous manifestations and complications of inherited epidermolysis bullosa: part I. Epithelial associated tissues. *J Am Acad Dermatol*. 2009;61: 367–384.
7. Destro M, Wallow IH, Brighthill FS. Recessive dystrophic epidermolysis bullosa. *Arch Ophthalmol*. 1987;105:1248–1252.
8. Motley WW, Vanderveen DK, West CE. Surgical management of infantile cataracts in dystrophic epidermolysis bullosa. *J AAPOS*. 2010;14:283–284.
9. Papathanassiou M, Petrou P, Papalexis G, Theodossiadis P. Intraoperative complication during phacoemulsification in patient with epidermolysis bullosa. *J Cataract Refract Surg*. 2011;37:198–200.
10. Lizio M, Harshbarger J, Shimoji H, et al. Gateways to the FANTOM5 promoter level mammalian expression atlas. *Genome Biol*. 2015;16:22.
11. Uechi G, Sun Z, Schreiber EM, Halfter W, Balasubramani M. Proteomic view of basement membranes from human retinal blood vessels, inner limiting membranes, and lens capsules. *J Proteome Res*. 2014;13:3693–3705.
12. Wullink B, Pas HH, Van der Worp RJ, Kuijer R, Los LI. Type VII collagen expression in the human vitreoretinal interface, corpora amylacea and inner retinal layers. *PLoS One*. 2015;10: e0145502.
13. Ponsioen T, van Luyn M, van der Worp R, van Meurs J, Hooymans J, Los L. Collagen distribution in the human vitreoretinal interface. *Invest Ophthalmol Vis Sci*. 2008;49: 4089–4095.
14. Tidman MJ, Eady RA. Ultrastructural morphometry of normal human dermal-epidermal junction. The influence of age, sex, and body region on laminar and nonlaminar components. *J Invest Dermatol*. 1984;83:448–453.
15. Banks WJ, Bale E, White FH. Morphometric studies of the epidermal-dermal junction in the rat ear: some effects of experimental friction on epidermis and anchoring fibrils. *J Anat*. 1984;139:425–435.
16. Janssen SF, Gorgels TG, Bossers K, et al. Gene expression and functional annotation of the human ciliary body epithelia. *PLoS One*. 2012;7:e44973
17. Hogan MJ, Alverado JA, Wedell JE. *Histology of the Human Eye: An Atlas and Textbook*. 1st ed. Philidelphia, Saunders; 1971:649.
18. Hanssen EE, Franc S, Garrone R. Synthesis and structural organization of zonular fibers during development and aging. *Matrix Biol*. 2001;20:77–85.
19. Raviola G. The fine structure of the ciliary zonule and ciliary epithelium. With special regard to the organization and insertion of the zonular fibrils. *Invest Ophthalmol*. 1971;10: 851–869.
20. Cain SA, Morgan A, Sherratt MJ, Ball SG, Shuttleworth CA, Kielty CM. Proteomic analysis of fibrillin-rich microfibrils. *Proteomics*. 2006;6:111–122.
21. Hiraoka M, Inoue K, Ohtaka-Maruyama C, et al. Intracapsular organization of ciliary zonules in monkey eyes. *Anat Rec (Hoboken)*. 2010;293:1797–1804.
22. Streeten BW. The zonular insertion: a scanning electron microscopic study. *Invest Ophthalmol Vis Sci*. 1977;16:364–375.
23. Kühl T, Mezger M, Hausser I, et al. Collagen VII half-life at the dermal-epidermal junction zone: implications for mechanisms and therapy of genodermatoses. *J Invest Dermatol*. 2016;136: 1116–1123.
24. Wenzel D, Bayerl J, Nyström A, Bruckner-Tuderman L, Meixner A, Penninger JM. Genetically corrected iPSCs as cell therapy for recessive dystrophic epidermolysis bullosa. *Sci Transl Med*. 2014;6264ra165.
25. Dayal JH, Cole CL, Pourreyron C, et al. Type VII collagen regulates expression of OATP1B3, promotes front-to-rear polarity and increases structural organisation in 3D spheroid cultures of RDEB tumour keratinocytes. *J Cell Sci*. 2014;127: 740–751.
26. Balasubramani M, Schreiber EM, Candiello J, Balasubramani GK, Kurtz J, Halfter W. Molecular interactions in the retinal basement membrane system: a proteomic approach. *Matrix Biol*. 2010;29:471–483.
27. De Maria A, Wilmarth PA, David LL, Bassnett S. Proteomic analysis of the bovine and human ciliary zonule. *Invest Ophthalmol Vis Sci*. 2017;58:573–585.
28. Zhang P, Kirby D, Dufresne C, et al. Defining the proteome of human iris, ciliary body, retinal pigment epithelium, and choroid. *Proteomics*. 2016;16:1146–1153.
29. Goel R, Murthy KR, Srikanth S, et al. Characterizing the normal proteome of human ciliary body. *Clin Proteomics*. 2013;10:9.
30. Cook JR, Carta L, Bénard L, et al. Abnormal muscle mechanosignaling triggers cardiomyopathy in mice with Marfan syndrome. *J Clin Invest*. 2014;124:1329–1339.


Investigative Ophthalmology & Visual Science